

ORIGINAL RESEARCH PAPER

Pages: 65-73

Modify the Injection Probe Equivalent Models by Considering the Shield Slot and Ferrite Permittivity Capacitors

Issa M. Mashriki¹, S.M.J. Razavi², S.H. Mohseni Armaki²¹High Institute for Applied Science and Technology, Syria.²Faculty of Electrical & Computer Engineering, Malek Ashter University of Technology, Iran, Tehran.

Issa_mashriki@mut.ac.ir, razavismj@mut.ac.ir, mohseni@mut.ac.ir

Corresponding Author: razavismj@mut.ac.ir

DOI: 10.22070/JCE.2022.15869.1207

Abstract- Explicit and hybrid equivalent models of bulk current injection probe are reviewed, these models don't take slot and ferrite dielectric constant capacitive effects into account, which cause the appearance of negative values in the real part of ferrite permeability spectra when extracting it from measured input impedance of the probe. In this paper, these capacitances are calculated using CST Electrostatic Solver, then its effect on the probe equivalent series impedance, voltage transfer ratio, and the core predicted permeability are evaluated. The evaluation shows that introducing these capacitances cancels the abnormal negative permeability resulting in the model, without affecting the model validation.

Index Terms- Bulk Current Injection (BCI) probe, Complex permeability spectra, Electromagnetic Compatibility (EMC), ferrite permittivity capacitance, slot capacitance.

I. INTRODUCTION

BCI probe is an immunity test device, when clamped on a wire harness it produces in it magnetic interference, its techniques have been accepted by about all regulatory standards [1]-[6].

The probe is shielded by two identical aluminum frames connected with the external connector from the outer side of the probe, and separated by a small slot from the inner side as shown in Fig.1. Thus the probe is partially shielded because of the slot existence, and that cannot be avoided, if so the probe would be loaded by a short circuit load.□

In [7], it was proved that changing the slot distance of the probe affects its measured reflection coefficient at high frequencies, which means that the slot existence contributes capacitively in its frequency response.□

□

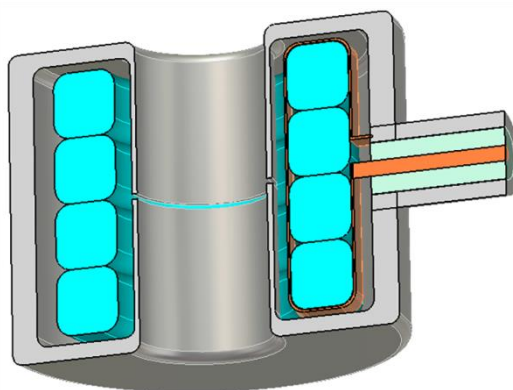


Fig. 1. A cross-sectional view of a BCI-probe.

The total value of the slot capacitor is usually small and is neglected at low frequencies, therefore, the slot is manipulated as an open circuit at low frequencies. At higher frequencies, the impedance of this capacitor decreases dramatically and its effect becomes meaningful, thus, its effect must be considered in any high-frequency circuitual model for the probe, and this is proved in this paper.

A resonance phenomenon, due to the dielectric constant in ferromagnetic materials, was observed in [8]. This paper shows that the capacitive effect resultant from ferrite dielectric constant in BCI-probe is much higher than that from the slot distance, even for nickel-zinc (NiZn) materials which are typically used in designing BCI-probes and characterized by low permittivity at high frequencies. Therefore, accurate modeling of BCI-probe can't be achieved without considering the effect of ferrite permittivity.

Accurate prediction of injection behavior helps in estimating and controlling RF interference levels, therefore, several research efforts have been done for modeling, analyzing, and characterizing the BCI probe [7], [9]-[11].

The explicit model derived in [9] and [10], which represents the base of later works such as in [12]-[14], doesn't take the slot capacitance and ferrite permittivity into account, just like the recently developed hybrid model [15]. Both models led to the appearance of negative real part permeability for the core when the permeability was extracted from measured input impedance using the model.

The complex permeability is the main parameter that defines the probe core material and is required for developing an accurate 2D or 3D model for the probe as in [16] and [17], or when the permeability spectra are introduced in the model as in [18], therefore, the circuit model must extract it accurately to get accurate results from the permeability based models.

The explicit model has been validated by comparing its equivalent series impedance and voltage transfer ratio with the implicit model extracted from measurements. Introducing the slot capacitance mustn't affect this validation; its effect must be restricted to the extracted permeability. In this paper, we will prove this claim while validating the developed model.

The explicit and hybrid models have the same magnetic coupling between the primary turn and the load and were validated, for the same BCI probe model F-130A, therefore reviewing one of them would be sufficient, then the suggested modifications could be applied for both of them in the same manner.

II. REVIEW OF THE EXPLICIT MODEL

The explicit model as proposed in [9] and its T-equivalent model are reported in Fig. 2. In which, ($L_1-M=0$) and ($L_2-M=L_{2d}$), where L_{2d} represents the leakage inductance and L_1 , L_2 and M denote the primary, secondary and mutual inductances between the probe and the clamped wire, respectively. Parameters C_N and L_N are used for modeling the connector with its adapter, while C_{w1} and L_{w1} denote the total capacitance and inductance between the primary winding and the probe frame.

From an electrical point of view, the probe is equivalent to a voltage source V_s with a series impedance Z_p . According to [9], these parameters can be extracted apart from measured S-parameters and could be calculated from Fig. 2 to validate the explicit model using (1)-(3).

$$V_s = \frac{sM \cdot V_{RF}}{s(L_1+L_{w1})+(R_s+sL_N)(1+s^2(C_N+C_{w1})(L_1+L_{w1}))} \quad (1)$$

$$Z_p = sL_{2d} + \frac{sMZ}{sM+Z} \quad (2)$$

$$Z = sL_{w1} + \frac{sL_N+R_s}{1+s(C_N+C_{w1})(sL_N+R_s)} \quad (3)$$

Where Z denotes the total primary impedance as seen from the primary coil. The voltage transfer ratio is defined by the quantity V_s/V_{RF} .

In [9], the model was validated first versus V_s/V_{RF} and Z_p for the probe model F-130A, then used for extracting the core complex permeability spectra apart from measured reflection coefficient S_{11} at the input of the probe without clamping it to a wire, i.e. after canceling the secondary coil circuit in the model of Fig. 2(a). This leads to the knowledge of the probe's input impedance Z_{in} which in turn leads to the knowledge of probe primary inductance L_1 and core permeability μ as

$$Z_{in}(\omega) = 50 \frac{1+S_{11}}{1-S_{11}} \quad (4)$$

$$Z_{L1} = j\omega\hat{L}_1(\omega) = \frac{1}{D}\{Z_{in}(\omega) - j\omega L_N\} - j\omega L_{w1} \quad (5)$$

$$D = 1 - j\omega(C_N + C_{w1})(Z_{in}(\omega) - j\omega L_N) \quad (6)$$

$$\hat{L}_1(\omega) = L_0(\mu'_r(\omega) - j\mu''_r(\omega)) \quad (7)$$

Applying the procedure for the probe F-130A led to extracting the permeability spectra of the core (black curve in Fig. 6). Reading the real part at the frequency of 100 MHz gives approximately $\mu'_{(100\text{MHz})} = -43$, physically, this value means that the coil can amplify the power or produces output

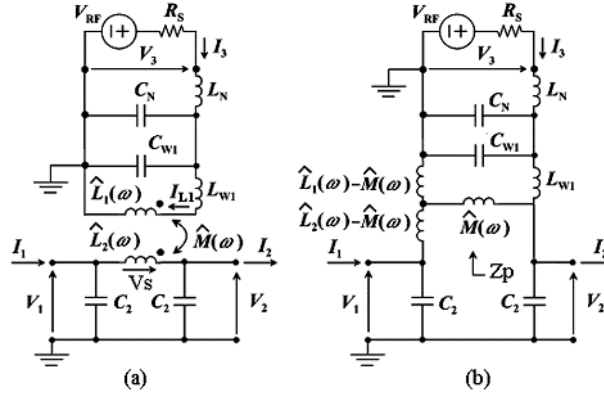


Fig. 2. Explicit lumped-parameter circuit model of the injection probe clamped onto the conductor under test (a) coupling model (b) T-equivalent model [10].

energy more than the input one at this frequency and this can't be achieved using only one source, another biasing source is needed to get this result.

The negative permeability was interpreted as due to dimensional resonance in large ferrite cores. The study in [8], proved that negative permeability can't be found in natural materials, like ferrite, even for big size cores, and that the dimensional resonance phenomenon is a matter of using low-frequency inductor's equivalent model for extracting the permeability spectra from measured input impedance at high frequencies, this let the resulted negative permeability without interpretation. In the following, we would show that negative permeability is a matter of non-considering some parameters in the model.

III. ILLUSTRATING THE EFFECT OF SLOT AND FERRITE PERMITTIVITY

A. Slot Effect

For illustrating the slot, four identical toroidal cores from NiZn material, with positive permeability at all frequencies [19], are used in implementing the BCI-probe shown in Fig. 3, the design intended to use the same primary winding and to achieve the same spaces between the core and the shield as that for F-130A. The result of measuring the amplitude of reflection coefficient for four different slot distances shown in Fig. 3, illustrates that the slot contributes to the frequency response of the probe and its effect must be considered in any high frequency equivalent model.

B. Ferrite Permittivity Effect

In [8], six toroidal cores, from the same material used in the previous section, were used for achieving the test of connector shifting, which illustrates the double resonance phenomenon resultant from the dielectric constant found in ferrite. The results of simulation and measurement of the imaginary part of input impedance show the appearance of two resonance frequencies, low f_L and high f_H . With

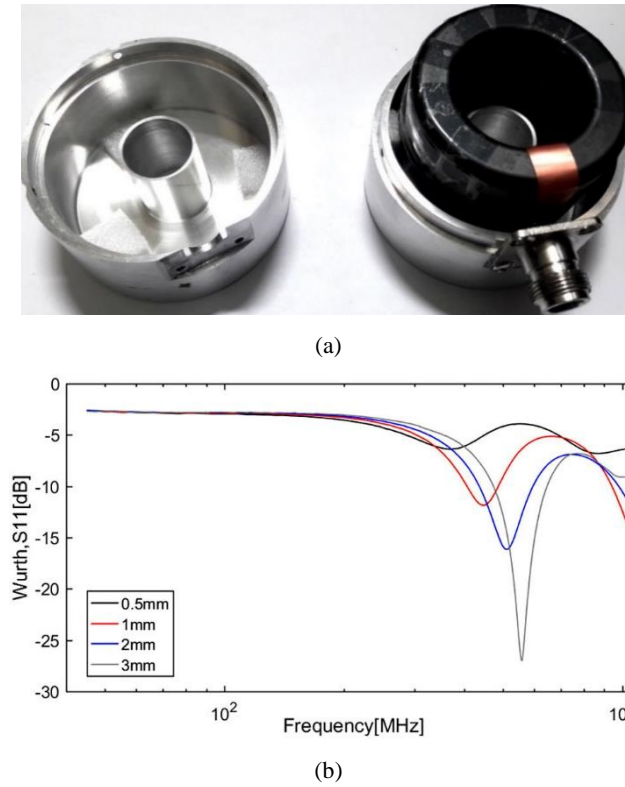


Fig. 3. (a) The probe, (b) Measured $|S_{11}|$ at the probe input for various slot distances (0.5, 1, 2, and 3 mm).

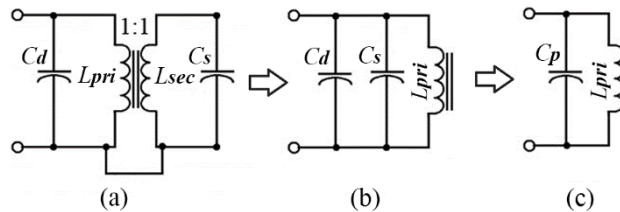


Fig. 4. Modeling the slot (C_s) and ferrite permittivity (C_d) capacitive effects: (a) basic, (b) transformed and (c) equivalent model.

respect to the middle location for the connector, f_L increases and f_H decreases when the connector is left-shifted, while f_L decreases and f_H increases when the connector is right-shifted. This proves that shifting the connector increases one of the two in-turn capacitors and decreases the other one. The material of used cores is NiZn, which has a low dielectric constant, therefore, the capacitive effect of the connector is comparable in compared with the in-turn capacitive effect resultant from the core permittivity. When MnZn has used the effect of dielectric permittivity would be dominant, the effect of shifting the connector would be more apparent and resonance would occur at lower frequencies.

IV. MODELING THE SLOT AND FERRITE PERMITTIVITY CAPACITANCES

The shield is seen by the primary turn as a secondary coil with a single turn loaded by the slot capacitance C_s , while the capacitive effect resultant from ferrite permittivity C_d appears in the

equivalent model as a parallel connection with the primary turn as shown in the basic model of Fig. 4 (a). When transformed to the primary, the slot capacitance can be represented in parallel with the primary turn, without changing its value, just as shown in Fig. 4 (b). Thus, both capacitors are replaced in the equivalent model by a single capacitor $C_p=C_s+C_d$ as shown in Fig. 4 (c).

V. ESTIMATING THE SLOT AND FERRITE PERMITTIVITY CAPACITANCES

A. Estimating The Slot Capacitance

Dimensions of the probe F-130A are reported in its manufacturer datasheet, and Appendix A of reference [10]. The problem of predicting the slot capacitance is simplified to the problem of predicting the capacitance between two axially centered cylindrical conductors spaced by a distance $d=1\text{mm}$.

In [7], it was proved that ferrite existence doesn't contribute to predicted slot capacitance even for high permittivity, therefore, the core would be ignored in the equivalent model used for estimating the slot capacitance of the probe F-130A. A cross sectional view of the model as implemented using CST-MWS software is shown in Fig. 5 (a), CST electrostatic solver is used in predicting the capacitance C_s and a value of 4.5 pF was obtained.

B. Ferrite Permittivity Capacitance

A rough evaluation for the value of ferrite permittivity capacitance (C_d) can be done, too, using CST Electrostatic Solver, in which the primary turn and the core are modeled as shown in Fig. 5 (b), the side parts of the turn are cut in the model. The upper two copper sections are connected to 1V while the bottom section is connected to the ground and the relative dielectric constant of the core is taken at 14 as in [20] for the probe F-130A, this value is close to that recorded from measurements for NiZn at high frequencies [21]. The result of the simulation gives a value of $C_d=6.4$ pF for the probe F-130A. The comparison between the value of predicted C_d and that of C_s illustrates that ferrite permittivity is more effective than the capacitive effect resultant from the slot capacitance, therefore, its contribution must be considered in the equivalent model of any BCI-probe.

VI. INTRODUCING THE SLOT CAPACITANCE IN THE EXPLICIT MODEL

In the explicit circuit model (Fig. 2), the total capacitor of $C_p=C_s+C_d =10.9$ pF are added in parallel with L_1 , and formulas (5) is altered accordingly by replacing Z_{L_1} with Z_{L_1}/Z_{C_p} , the predicted complex permeability spectra resultant from this modification (gray curves), in comparison with the precedent case (black curve), are shown in Fig. 6. The result of comparing the real part (dashed curves), illustrates that adding C_p cancels the negative real permeability resulting in the basic model.

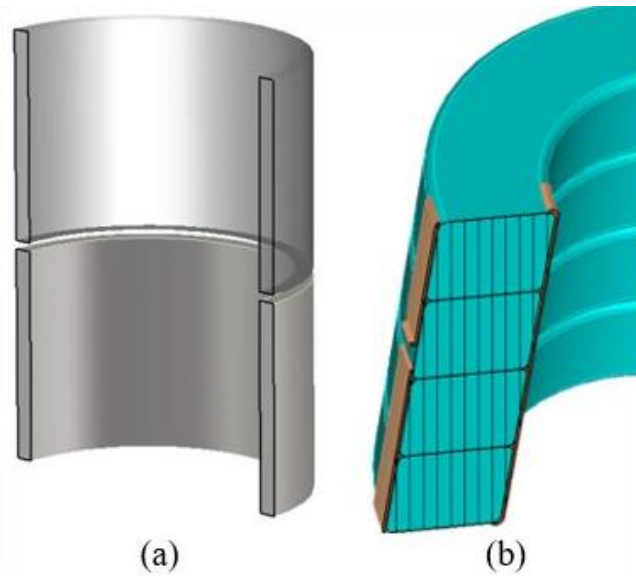


Fig. 5. A cross sectional view of the CST-model used in predicting the (a) C_s and (b) C_d of BCI-probe model F-130A.

The same modification can be applied to the hybrid model and gives the same result. This disclosed the reason behind the negative real permeability appearance in the basic models and is interpreted as a result of neglecting the slot and ferrite permittivity capacitive effect.

Simulation in MATLAB shows that introducing C_p doesn't make any change in the series impedance spectra after altering the expression in (2), to take it into regard. This can be proved analytically as follow: since ($L_1=M$) and the impedance of the primary inductance Z_{L1} before introducing C_p , is equal to the impedance $Z_{L1} // Z_{Cp}$ for primary inductance in parallel with C_p after introducing it, this equality is because the two cases have the same measured input impedance.

Also, the voltage transfer ratio doesn't suffer any changes when C_p is introduced in (1), this is because the voltage between the two ends of the primary inductance doesn't change by introducing C_p in parallel with it. Thus adding C_p doesn't affect the validation of explicit and hybrid models, and its effect appears just in the extracted complex permeability of the core.

The injection probe F-130A was not available for verification, but measurements were made with two types of BCI probes with different ferrite samples and reported in [7]. The results of the investigation of the imaginary part of the measured input impedance show that inductive and capacitive regions appear sequentially and the reduction of slot capacitance causes the shift of the curve towards higher frequencies. To determine the range limit of frequencies at which the slot capacitance contribute the input impedance, its effect is canceled by making the slot distance big

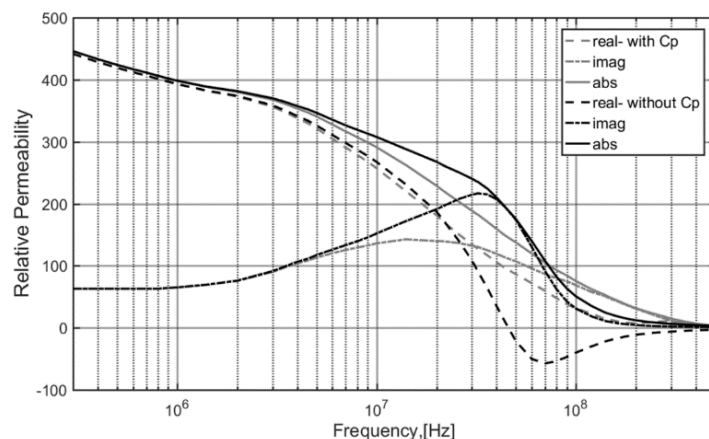


Fig. 6. Complex permeability spectra of the ferrite core of the injection probe F-130A with and without [10] introduce the total capacitance C_p in the explicit model.

enough. When the slot capacitance is omitted the second and third inductive regions combines together as in measurement, which assures that they have the same source parameters.

Investigated input impedance indicates that ferrite permittivity is responsible for a capacitive contribution at all the measuring bandwidth, this reveals the role of permittivity in magnetic devices as introducing capacitive influence, which results in a resonance phenomenon in the device.

□

VI. CONCLUSION

The capacitive effects resultant from the slot and ferrite permittivity on the BCI probe model FCC-F-130A were studied, their values were predicted using CST Electrostatic Solver and introduced in the state-of-the-art equivalent models without making any change in the other elements arrangement and their values. The effect of these capacitances on the explicit model derived in [10] showed that introducing these capacitances doesn't change the equivalent series impedance and voltage transfer ratio employed in validating the model but improves the extracted permeability spectra of the core by canceling the abnormal negative real permeability at all the probe working frequencies. This discloses the reason behind getting a negative value in permeability spectra when extracting it from measured input impedance and disproves interpreting it as a result of dimensional resonance phenomena in large-size cores.

REFERENCES

- [1] RTCA/DO-160D- "Environmental conditions and test procedures for airborne equipment," CYTEC Corporation, July, 1997.
- [2] Electromagnetic compatibility (EMC) -Part4-6: Testing and measurement techniques- Immunity to conducted disturbances, induced by radio-frequency fields, IEC Standard 61000-4-6, May 2006.

- [3] ISO Standard 11451-4: Road Vehicles-Vehicle test methods for electrical disturbances from narrowband radiated electromagnetic energy-Part4: Bulk Current Injection (BCI), June, 2006.
- [4] ISO Standard 11452-4: Road Vehicles- Component Test Methods for Electrical Disturbances from Narrowband Radiated Electromagnetic Energy-Part4: Harness excitation methods, Dec.2011.
- [5] IEC 62132-3, Ed.1: Integrated Circuit Measurements of Electromagnetic Immunity 150kHz to 1GHz, Part 3: Bulk Current Injection (BCI) Method, 2007.
- [6] Department of Defense Interface Standard, "Requirements for the Control of Electromagnetic Interference Characteristics of Subsystems and Equipment," MIL-STD-461E, Aug. 20, 1999.
- [7] Issa M. Mashriki, S.M.J. Razavi, and S.H.M. Armaki, "Analyzing the Resonance Resultant from the Capacitive Effects in Bulk Current Injection Probe," *Radioengineering*, vol.29, no.1, pp. 109-116, April 2020.
- [8] Issa M. Mashriki, S.M.J. Razavi, and S.H.M. Armaki, "In-turn capacitive effect resultant from a high dielectric constant found in a ferromagnetic ferrite," *Int. Journal Electron. Commun. (AEÜ)*, vol.124, 15335, Sept. 2020.
- [9] F. Grassi, S.A. Pignari, and F. Marliani, "Improved lumped-Pi circuit model for bulk current injection probes," in *Proc. IEEE Symp. Electromagn. Compat.*, Chicago, IL, Aug. (8–12) 2005, pp.451–456.
- [10] F. Grassi, F. Marliani, and S.A. Pignari "Circuit Modeling of Injection Probes For Bulk Current Injection," *IEEE Trans. Electromagnetic. Compatibility.*, vol.49, no.3, pp.563-576, Aug.2007.
- [11] F. Grassi, S.A. Pignari, and G. Spadacini, "Time-Domain Response of Bulk Current Injection Probes to Impulsive Stress Waveforms," *IEEE. Conf. Dresden*, Germany, Aug. 2015.
- [12] Flavia Grassi, "Accurate Modeling of Ferrite-Core Effects in Probes for Bulk Current Injection," in *Proc. 2009 IEEE Int. Conf. on Microw., Commun., Antenna and Elec. Systems, IEEE COMCAST*, Nov. 2009, pp.1-6.
- [13] Wenjing Zhao, Zhaowen Yan, and Wei Liu, "Two methods for BCI probe to improve the high frequency performance," *IEEE, 11th International Symposium on Antennas, Propagation and EM Theory (ISAPE)*, Oct. 2016.
- [14] F. Grassi and S.A. Pignari, "Bulk current injection in twisted wire pairs with not perfectly balanced terminations," *IEEE Trans. Electromagn. Compat.*, vol. 55, no. 6, pp. 1293-1301, Dec. 2013.
- [15] Issa M. Mashriki, S.M.J. Razavi, S.H.M. Armaki, "Hybrid model for Bulk Current Injection Probe," *Journal of Communication Engineering*, vol. 8, no. 2, pp. 277-289, July-December 2020.
- [16] M.S. Diop, E. Clavel, H. Cheaito, C. Vollaïre, and E. Vialardi, "2D modeling of Bulk Current Injection Probe and Validation with Measurements," 32nd General Assembly and Scientific Symposium of the International Union of Radio Science (URSI GASS), Montreal, 19-26 August 2017.
- [17] P. DeRoy and S. Piper, "Full-wave Modeling of Bulk Current Injection Probe Coupling to Multi-conductor Cable Bundles," *IEEE International Symposium on Electromag. Compatib.*, July 2016.
- [18] F.Grassi, F.Marliani, and S.A.Pignari, "SPICE modeling of BCI probes accounting for the frequency-dependent behavior of the ferrite core," in *Proc. XIXth General Assembly of International Union of Radio Science (U. R.S. I)*, Chicago, IL, USA, pp. 7-16, August 2008.
- [19] Fair-Rite_Catalog_17th_Edition, Fair-Rite Products Corp
- [20] Nicola Toscani, Flavia Grassi, Giordano Spadacini, Sergio A.Pignari, "Circuit and Electromagnetic Modeling of Bulk Current Injection Test Setups Involving Complex Wiring Harnesses," *IEEE Trans. Electromagnetic Compatibility*, vol. 60, no. 6, pp. 1752-1760, Dec. 2018
- [21] K.R. Krishna1, D. Ravinder, K.V.Kumar, U.S.Joshi, and V.A.Rana, A.Lincon, "Dielectric Properties of Ni-Zn Ferrites Synthesized by Citrate Gel Method," *World Journal of Condensed Matter Physics*, vol. 2, pp. 57-60, 2012.